Anal. Chem. **2003,** *75,* 5495−5503

High-Precision Position-Specific Isotope Analysis of $^{13}C/^{12}C$ in Leucine and Methionine Analogues

Gavin L. Sacks and J. Thomas Brenna*

Division of Nutritional Sciences, Savage Hall, Cornell University, Ithaca, New York 14853

We report an automated method for high-precision position-specific isotope analysis (PSIA) of carbon in amino acid analogues. Carbon isotope ratios are measured for gas-phase pyrolysis fragments from multiple sources of 3-methylthiopropylamine (3MTP) and isoamylamine (IAA), the decarboxylated analogues of methionine and leucine, using a home-built gas chromatography (GC)-pyrolysis-GC preparation system coupled to a combustion-isotope ratio mass spectrometry system. Over a temperature range of 620−900 °C, the characteristic pyrolysis products for 3MTP were CH_4, C_2H_6, HCN, and CH_3CN and for IAA products were propylene, isobutylene, HCN, and CH_3CN. Fragment origin was confirmed by ^{13}C-labeling, and fragments used for isotope analysis were generated from unique moieties with >95% structural fidelity. Isotope ratios for the fragments were determined with an average precision of SD($\delta^{13}C$) < 0.3‰, and relative isotope ratios of fragments from different sources were determined with an average precision of SD($\Delta\delta^{13}C$) < 0.5‰. $\Delta\delta^{13}C$ values of fragments were invariant over a range of pyrolysis temperatures. The $\Delta\delta^{13}C$ of complementary fragments in IAA was within 0.8‰ of the $\Delta\delta^{13}C$ of the parent compounds, indicating that pyrolysis-induced isotopic fractionation is effectively taken into account with this calibration procedure. Using $\Delta\delta^{13}C$ values of fragments, $\Delta\delta^{13}C$ values were determined for all four carbon positions of 3MTP and for C1, C2, and the propyl moiety of IAA, either directly or indirectly by mass balance. Large variations in position-specific isotope ratios were observed in samples from different commercial sources. Most dramatically, two 3MTP sources differed by 16.30‰ at C1, 48.33‰ at C2, 0.37‰ at C3, and 5.36‰ at C(methyl). These PSIA techniques are suitable for studying subtle changes in intramolecular isotope ratios due to natural processes.

High-precision isotope ratio analysis is presently used across the natural sciences for an increasing array of applications.[1] Bulk stable isotope analysis (BSIA) of $\delta^{13}C$ and $\delta^{15}N$ in complex natural solids and compound-specific isotope analysis (CSIA) of volatile compounds are automated and routine;[2] the analytical frontier now lies in the development of automated position-specific isotope analyses (PSIA) for intramolecular analysis.

We have previously suggested that intramolecular isotope ratios should be sensitive to the physiology of the organism that synthesizes them and that isotope ratios are potentially of wide utility as markers of physiological state.[3] Intramolecular isotope ratios should be especially sensitive to shifts in metabolism because isotope fractionation is localized to carbon sites associated with the rate-determining step of a particular metabolic process. Position-specific studies can therefore focus on the atomic positions that show the greatest susceptibility to isotope fractionation without dilution from the rest of the molecule. PSIA studies also offer an extended source of isotopic information since the isotope ratio at each site is a composite of fractionations associated with elementary (bio)chemical steps involved in the synthesis and degradation of molecules.

Over several years, strategies based on isotope ratio mass spectrometry (IRMS)[4] and on NMR[5] have been introduced for high-precision intramolecular analysis. We have previously described a system that coupled a tandem gas chromatograph (GC) to a pyrolysis furnace (Py). Fragments were converted to CO_2 in a combustion furnace, and characterized isotopically by IRMS. Using this GC-Py-GCC-IRMS system, we have presented results exploiting pyrolytic fragmentation for PSIA of several classes of compounds, including fatty acid methyl esters,[4] fatty alcohols,[6] and *n*-alkanes.[7] We have shown with labeling studies that open tube pyrolysis of these compounds does not scramble carbon positions while also producing high-precision isotope ratios of stabilized neutral fragments. Yamada et al. have recently extended this work to PSIA studies of acetate.[8]

The amino acids are attractive candidates for high-precision carbon isotope analysis due to their ubiquity as protein building blocks and their myriad functions in metabolic processes. Carbon isotope signatures in amino acids have been used to investigate the origin of organic material in meteorites,[9] the symbiotic

* Corresponding author. E-mail: jtb4@cornell.edu. Phone: (607) 255-9182. Fax: (607) 255-1033.

(1) Asche, S.; Michaud, A. L.; Brenna, J. T. *Curr. Org. Chem.*, in press.
(2) Meier-Augenstein, W. *J. Chromatogr., A* **1999**, *842*, 351−371.
(3) Brenna, J. T. *Rapid Commun. Mass Spectrom.* **2001**, *15*, 1252−1262.
(4) Corso, T. N.; Brenna, J. T. *Proc. Natl. Acad. Sci. U.S.A.* **1997**, *94*, 1049−1053.
(5) Zhang, B. L.; Buddrus, S.; Martin, M. L. *Bioorg. Chem.* **2000**, *28*, 1−15.
(6) Corso, T. N.; Lewis, P. A.; Brenna, J. T. *Anal. Chem.* **1998**, *70*, 3752−3756.
(7) Corso, T. N.; Brenna, J. T. *Anal. Chim. Acta* **1999**, *397*, 217−224.
(8) Yamada, K.; Tanaka, M.; Nakagawa, F.; Yoshida, N. *Rapid Commun. Mass Spectrom.* **2002**, *16*, 1059−1064.
(9) Engel, M. H.; Macko, S. A.; Qian, Y.; Silfer, J. A. In *Life Sciences and Space Research XXV (4)*; Cogoli, A., et al., Eds.; Committee on Space Research; Pergamon: New York, 1994; Vol. 15, pp 99−106.

10.1021/ac0344889 CCC: $25.00
Published on Web 08/30/2003

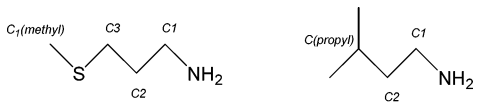

I II

Figure 1. Structures of 3MTP (**I**) and IAA (**II**).

relationship between plankton and algae,[10] and the role of microbes in soil.[11] The earliest PSIA study was performed on amino acids[12] and used off-line decarboxylation to demonstrate that the carboxyl position of amino acids is enriched with respect to the rest of the molecule and that the degree of enrichment depends on the organism from which it is derived.

Pyrolytic decomposition proceeds primarily by free-radical chain mechanisms, which often lead to fragment patterns fundamentally different from the electron impact mass spectra of the same compounds.[13] Hydrocarbon pyrolysis is described well by modified Rice theory,[14] which predicts an initial bond cleavage to form free radicals, followed by propagation and stabilization by the loss of neutral olefins to form smaller free radicals, or termination by the recombination of two free radicals. For intramolecular comparisons, pyrograms should ideally contain fragments with well-defined origins. Thus, the pyrolysis temperature is chosen not only to maximize signal level but also to produce characteristic pyrograms which contain fragments that arise from specific locations. We use the term *structural fidelity* to describe fragments that originate from unique positions in the parent molecule. Our previous work has shown that methyl palmitate labeled in the methyl and terminal carbons shows no pyrolysis-induced rearrangement.[4] However, that work was concerned primarily with long-chain fragments (C_n, $n > 3$). Small fragments such as CH_4 may result from either primary or secondary fragmentation and, therefore, are more likely to be formed from multiple sites within the parent molecule. Method development for PSIA involving small fragments requires optimal chromatography, fragment identification, and confirmation of structural fidelity.

Amino acids are nonvolatile and thus incompatible with GC analysis. Decarboxylation is an attractive alternative to other derivatization schemes that add exogenous carbon and would likely interfere with the fidelity of pyrolysis fragments.[15] In this report, we develop a method for PSIA studies for the decarboxylated analogues of two amino acids (Figure 1): 3-methylthiopropylamine (3MTP), the analogue of methionine (**I**), and isoamylamine (IAA), the analogue of leucine (**II**). We describe the effects of varying pyrolysis temperatures on the distribution and nature of pyrolysis fragments and optimize methods for obtaining fragments representative of specific positions in the parent compound. Finally, we report $\delta^{13}C_{PDB}$ values of the fragments resulting from the pyrolysis of four different commercial sources of the analogues and use these values to show intramolecular isotope ratio differences ($\delta\Delta^{13}C$) between the sources.

(10) Uhle, M. E.; Macko, S. A.; Spero, H. J.; Engel, M. H.; Lea, D. W. *Org. Geochem.* **1997**, *27*, 103−113.
(11) Glaser, B.; Amelung, W. *Rapid Commun. Mass Spectrom.* **2002**, *16*, 891−898.
(12) Abelson, P. H.; Hoering, T. C. *Proc. Natl. Acad. Sci. U.S.A.* **1961**, *47*, 623−632.
(13) Kelley, J. D.; Wolf, C. J. *J. Chromatogr. Sci.* **1970**, *8*, 583−585.
(14) Rice, F. O. *Collected Papers of F. O. Rice*; Catholic University of America Press: Washington, DC, 1958.
(15) Zaideh, B. I.; Saad, N. M. R.; Lewis, B. A.; Brenna, J. T. *Anal. Chem.* **2001**, *73*, 799−802.

EXPERIMENTAL SECTION

GC-Py-GCC-IRMS System and Data Processing. The on-line pyrolysis system consists of a home-built GC-pyrolysis-GC interface coupled to a continuous-flow combustion/high-precision IRMS, described in detail elsewhere.[4] Briefly, two commercial capillary GCs (GC-1, HP 5890, Palo Alto, CA; GC-2, Varian, Inc. 3400, Walnut Creek, CA) were linked via a pyrolysis reactor. The sample was injected, splitless, via an autosampler (Varian 8200) into GC-1, and components were separated on a 30 m × 0.32 mm × 5.0 μm DB-1 capillary column (cross-linked dimethylpolysiloxane; Agilent Technologies, Palo Alto, CA). The initial GC-1 oven temperature was 100 °C, held for 5 min, ramped to 200 °C at 20 °C/min, and held for 20 min. The head pressure was set at 25 psi, resulting in a flow velocity through GC-1 and GC-2 of 30 cm/s. The GC-1 column was connected to an automated rotary valve (Valco, Houston, TX), which led to either (a) a flame ionization detector (FID), for determining retention times, or (b) the pyrolysis-GC system. Using the FID retention times, the rotary valve was programmed to select a single component for pyrolysis from the eluent stream.

The pyrolysis reactor consisted of a single piece of 0.32-mm fused-silica capillary tubing positioned such that effluent entered from the GC-1 rotary valve, traveled sequentially through a heated transfer line, a 20-cm-long pyrolysis furnace zone, and finally another heated transfer line into GC-2, where it connected to a second capillary column. The fused silica was anchored to a ceramic tube inside the pyrolysis furnace for mechanical support. The pyrolysis zone was resistively heated by a Fibercraft furnace (Thermcraft, Winston-Salem, NC), and the temperature was controlled to ±0.5 °C by a CN9000A series temperature controller (Omega Engineering, Stamford, CT).

Following pyrolysis, fragments were directed to GC-2 for separation by a 30 m × 0.32 mm × 1.5 μm GS-CarbonPLOT column (Agilent). The GC-2 oven was held at 30 °C for 2−4 min past the retention time of the analyte to capture all pyrolysis products. The oven was ramped to 70 °C at 50 °C/min, ramped to 90 °C at 3 °C/min and held for 5 min, ramped to 140 °C at 50 °C/min, and finally, ramped to 200 °C at 5 °C/min and held for 5 min. After the fragments were separated, they were directed by a second rotary valve for either isotopic or molecular analysis. For isotopic analysis, the fragments entered a home-built combustion furnace/Nafion water trap interface coupled via an open split to a Finnigan-MAT 252 (Bremen, Germany) operating in high-stability mode for high-precision isotope analysis. The combustion reactor consisted of a 30-cm-long, 0.5-mm-i.d. ceramic tube, packed with oxidized Cu, and resistively heated to 950 °C by a second Fibercraft furnace. For molecular analysis, fragments entered a Varian Saturn III QISMS ion trap operated in positive ion electron impact mode. Ion trapping is inefficient at $m/z < 20$, so the identification of CH_4 was confirmed by retention time using a standard. Interpretation of spectra on the QISMS ion trap was aided by the Wiley mass spectral database (Palisades, Newfield, NY). For isotope analysis of the parent compounds (CSIA), the column in GC-2 was replaced with a 1 m × 0.32 mm fused-silica

transfer line, and the oven was held at 200 °C. The pyrolysis furnace was set to 300 °C, well below the threshold for observable pyrolysis.

Consecutive GC-Py-GCC-IRMS runs were performed using SAXICAB,[16] a home-written LabVIEW 6i[17] software for continuous-flow IRMS automation. SAXICAB allows for automated control of most GC-Py-GCC-IRMS parameters during a run, including injecting the sample, triggering the GC ovens, switching the GC-1 rotary valve, setting the pyrolysis furnace temperature, and introducing standard pulses. Data were collected from the IRMS using high-precision NI435x data acquisition boards (National Instruments; Austin, TX). $\delta^{13}C_{pdb}$ values were also calculated by SAXICAB. We have previously demonstrated that SAXICAB achieves accuracy and precision identical to that of the proprietary ISODAT (Finnigan MAT; Bremen, Germany) software.[16] Smaller peaks were integrated by curve fitting the three traces ($^{44}CO_2$, $^{45}CO_2$, $^{46}CO_2$) to an exponentially modified Gaussian function. The fit was optimized by the Levenberg−Marquardt algorithm using native LabVIEW functions. Previous work has shown that curve fitting achieves better accuracy and precision than traditional summation methods for small[18] and overlapping[19] peak areas. Larger peaks often displayed distorted peak shape, which interfered with curve fitting; large peak areas were instead calculated by the familiar method of summing the ion current over the width of the peak. The "dynamic" summation algorithm, as outlined by Ricci,[20] was used to correct the CO_2 background when the summation method was used. For both curve-fitting and summation, $\delta^{13}C$ was calculated using the method of Santrock et al.,[21] to account for the contribution of the ^{17}O concentration to the $m/z = 45$ signal.

Amino Acid Analogue Samples. The amino acid analogues were acquired commercially either "as is" or as amino acids and decarboxylated. The latter was necessary due to the scarcity of commercial sources for either natural abundance or ^{13}C-labeled amino acid analogues. The decarboxylation procedure was adapted from Hashimoto et al.[22] Briefly, the amino acid (2 g) was added to 10 mL of a 1% solution of 2-cyclohexen-1-one (95%+, Sigma-Aldrich; St. Louis, MO) in cyclohexanol (99%, Fluka; Buchs, Switzerland) and heated to reflux for 5 h. The reaction mixture was diluted with methanol to form a 2 mg/mL solution of the analogue prior to GC-Py-GCC-IRMS analysis, without further isolation or purification. Yields were >60% for both amino acids.

Four sources of 3MTP (designated E, F, G, H) and three sources of IAA (L, M, N), shown in Table 1, were studied by GC-Py-GCC-IRMS. For the labeling experiments, [C(methyl)-^{13}C]-3MTP was generated by decarboxylation of [C(methyl)-^{13}C]-methionine, and [1-^{13}C]-IAA was generated by decarboxylation of [2-^{13}C]-leucine. Both labeled amino acids were purchased from Cambridge Isotope Laboratories (99%; Andover, MA).

Table 1. Sources of 3MTP and IAA Used in This Work[a]

	source	compound/manufacturer	prep
3MTP	E	DL-methionine from J. T. Baker (99%; Phillipsburg, NJ)	De−CO_2
	F	L-methionine from Avocado RC, Ltd. (99%; Heysham, England)	De−CO_2
	G	L-methionine from Acros (99%; Geel, Belgium)	De−CO_2
	H	3MTP from Acros (97%; Geel, Belgium)	Used as is
IAA	L	L-leucine from Acros (99%; Geel, Belgium)	De−CO_2
	M	IAA from Aldrich (99%; St. Louis, MO)	used as is
	N	IAA from Acros (99%; Geel, Belgium)	used as is

[a] Abbreviations in the left-most column are used in the rest of the paper.

Reporting Intramolecular Isotope Ratios. The accepted method for reporting isotope measurements in CSIA and BSIA studies is to compare the isotope ratio of the analyte to the isotope ratio of a standard. For carbon studies, analytes are indirectly calibrated against PeeDee Belemnite (PDB) and expressed in delta notation:

$$\delta^{13}C_{PDB} = \frac{R_{spl} - R_{PDB}}{R_{PDB}} \times 1000; \quad R_x = \left[\frac{^{13}C_x}{^{12}C_x}\right] \qquad (1)$$

where R_{spl} is the isotope ratio of the sample. Isotope ratios are normally calibrated by analysis of sample followed by analysis of a working standard calibrated ultimately against PDB. Routinely the isotopic standard is CO_2 gas admitted to the analysis stream via a special reference gas injector. Implicitly, this procedure takes into account fractionation that would be inconvenient to characterize, for example, fractionation that occurs in the IRMS ion source and detectors. In PSIA, the degree of fragmentation in the pyrolysis furnace provides an additional source of fractionation. $\delta^{13}C_{pdb}$ values of fragments are inherently meaningful only in the case of quantitative pyrolysis, which has been verified in some cases (e.g., ref 7). However, as shown below, partial pyrolysis is usually necessary to ensure the fidelity of a fragment's origin, and isotopic fractionation always occurs under these circumstances. The CO_2 gas standard is not subject to this fractionation, and thus reporting $\delta^{13}C$ relative to the standard is not inherently meaningful. The solution is to report *relative* differences ($\Delta\delta^{13}C$) in intramolecular isotope ratios among comparable positions in a series of samples. Instead of comparing isotope ratios to a pulse of standard CO_2 gas, the isotope ratios of the analogous fragments from a sample compound are compared to the fragments from a standard compound run immediately before or after under identical conditions. This approach, which we adopt here, is functionally analogous to calibration of CO_2 samples against CO_2 standards.

Pyrolysis of small molecules causes isotopic fractionation due to kinetic isotope effects. In GC-Py-GCC-IRMS, the isotope ratio of the fragment, $^{13}R_{Fragment}$, is measured and is representative of the isotope ratio at a site or moiety before fragmentation, $^{13}R_{Moiety}$.

(16) Sacks, G. L.; Brenna, J. T.; Sepp, J. T. *49th ASMS Conference on Mass Spectrometry*, Chicago, IL, 2001.
(17) National Instruments, Austin, TX, 2000.
(18) Goodman, K. J.; Brenna, J. T. *J. Chromatogr., A* **1995**, *689*, 63−68.
(19) Goodman, K. J.; Brenna, J. T. *Anal. Chem.* **1994**, *66*, 1294−1301.
(20) Ricci, M. P.; Merritt, D. A.; Freeman, K. H.; Hayes, J. M. *Org. Geochem.* **1994**, *21*, 561−571.
(21) Santrock, J.; Studley, S. A.; Hayes, J. M. *Anal. Chem.* **1985**, *57*, 1444−1448.
(22) Hashimoto, M.; Eda, Y.; Osanai, Y.; Iwai, T.; Aoki, S. *Chem. Lett.* **1986**, 893−896.

This relationship may be written as

$$^{13}R_{Fragment} = \alpha(T,L,f,...)^{13}R_{Moiety} \quad (2)$$

where α is the fractionation factor, which is dependent on the temperature (T), the length of the furnace (L), the flow rate through the furnace (f), and innumerable other parameters. Note that no equivalent linear relationship can be written to relate the isotope fraction, ^{13}F, of the reactants to the products. The ratio of ratios between the sample (R_{spl}) and standard (R_{std}) isotope ratios for a fragment is

$$\left[\frac{^{13}R_{spl}}{^{13}R_{std}}\right]_{\substack{\text{observed}\\ \text{pyrolysis}\\ \text{fragments}}} = \frac{\alpha_{Spl}}{\alpha_{Std}} \cdot \left[\frac{^{13}R_{spl}}{^{13}R_{std}}\right]_{\substack{\text{fragments in}\\ \text{unpyrolyzed}\\ \text{compound}}} \quad (3)$$

If the sample and the standard are run under identical pyrolysis conditions, then their respective fractionation factors are equal. Equation 3 may be rewritten:

$$\frac{^{13}R_{spl}(\text{fragment})}{^{13}R_{std}(\text{fragment})} = \frac{^{13}R_{spl}(\text{original site})}{^{13}R_{std}(\text{original site})} \quad (4)$$

Thus, the ratio of isotope ratios for a fragment from a sample source with respect to a fragment from a standard source remains invariant with changes in pyrolysis conditions and is therefore appropriate for studying intramolecular isotopic variation. Because CSIA and BSIA data are reported in terms of $\delta^{13}C_{pdb}$, we find it more useful to express eq 4 using the "per mil" (‰) framework:

$$\left(\frac{^{13}R_{spl}}{^{13}R_{std}} - 1\right) \times 1000 = \delta^{13}C_{pdb}(spl) - \delta^{13}C_{pdb}(std) + \left(\frac{^{13}R_{spl}}{^{13}R_{std}} - 1\right) \times \delta^{13}C_{pdb}(std) \quad (5)$$

The ^{13}R's in eq 5 may refer to a fragment, a site, or the total compound. If the sample and standard isotope ratios are near natural abundance, then the final term will tend toward zero, and we can write

$$\Delta\delta^{13}C(spl) = \left(\frac{^{13}R_{spl}(\text{fragment})}{^{13}R_{std}(\text{fragment})} - 1\right) \times 1000 \quad (6)$$

$$\Delta\delta^{13}C(spl) = \delta^{13}C_{pdb}(spl) - \delta^{13}C_{pdb}(std) \quad (7)$$

$\Delta\delta^{13}C$ is therefore the per mil (‰) difference of analogous sites or fragments from two different sources of the same compound. This is similar to the concept of "Δ" used by Rieley to describe changes in $\delta^{13}C$ as a result of fractionation during the derivatization of organic compounds.[23]

To summarize, the relative isotope ratio of a fragment or site from a sample compound can be accurately reported as $\Delta\delta^{13}C$, the difference between the $\delta^{13}C_{pdb}$ of the sample fragment/site and the $\delta^{13}C_{pdb}$ of the same fragment/site from a standard compound as shown in eq 7. Assuming the sample and standard are analyzed under identical circumstances, and all values are near natural abundance, $\Delta\delta^{13}C$ should be independent of the pyrolysis conditions.

There is no well-established notation for designation of the site to which specific $\Delta\delta^{13}C$ value refers. As a convention in this report, the name of the standard is written in subscript, and the identity of the fragment or site is enclosed in parentheses afterward. Here we arbitrarily choose source N (for IAA) and source H (for 3MTP) as standards. As an example, the expression "$\Delta\delta^{13}C_H(HCN) = 13.22‰$ for source E", means that the HCN fragment generated from E is enriched by 13.22‰ with respect to the H standard. By definition, $\Delta\delta^{13}C_{Std}(X) = 0$ for any fragment or site, X, produced from a standard, Std.

The variance of $\delta^{13}C$ for the standard and the source were assumed to be independent. Propagation of errors for $\Delta\delta^{13}C$ was calculated through standard methods. Statistical analysis to compare $\Delta\delta^{13}C$ and $\delta^{13}C$ from different conditions was performed by the two-tailed t-test at the 95% confidence level ($p < 0.05$), using standard statistical tables.

RESULTS AND DISCUSSION

GC-Py-GCC-IRMS of 3MTP was performed at pyrolysis temperatures of 620, 660, 700, 740, 780, 820, 860, and 900 °C and on IAA at 700, 740, 780, 820, 860, and 900 °C to establish optimal fragmentation conditions. Once molecular structure was determined, the optimal pyrolysis temperature was established for each fragment such that the signal was maximal while the fragments were derived with high structural fidelity. Because a PLOT column was chosen for GC-2 to optimize resolution of the low molecular weight fragments, larger fragments and the 3MTP parent eluted only at very high temperatures among a background of high column bleed and were not analyzed isotopically.

Fragmentation Patterns and Fragment Origin. Pyrograms of IAA and 3MTP show some similar fragments (C_2H_4, HCN, CH_3-CN), as well as other fragments specific to each amino acid analogue. Representative IRMS pyrograms are shown in Figure 2. The distribution of fragments for both analogues at increasing pyrolysis temperatures is shown in Figure 3. The plot is in terms of "% molar conversion", the molar ratio of fragment detected to parent compound injected. This value will range from 0 to 100% for fragments generated with ideal structural fidelity but can be greater than 100% for fragments such as C_2H_4 that are generated from multiple locations. Generally, fragmentation does not occur below 600 °C, increases markedly in the range of 700−780 °C, and plateaus or decreases above 780 °C. This decrease at high pyrolysis temperatures is likely due to decomposition of the fragments to graphite and hydrogen.[24]

To assess the origin of fragments, 3MTP was labeled at the C(methyl) site, and IAA was labeled at the C1 position, according to numbering shown in Figure 1. ^{13}C-Labeled standards at three nominal enrichments ($\delta^{13}C_{pdb} = 0$, 200, and 400‰) were analyzed to identify the origin of fragments from within the parent molecule, where the δ value refers to the enrichment at the labeled site. The observed isotope ratio of a fragment can be expressed as a

(23) Rieley, G. *Analyst* **1994**, *119*, 915−919.

(24) Sofer, Z. *Anal. Chem.* **1986**, *58*, 2029−2032.

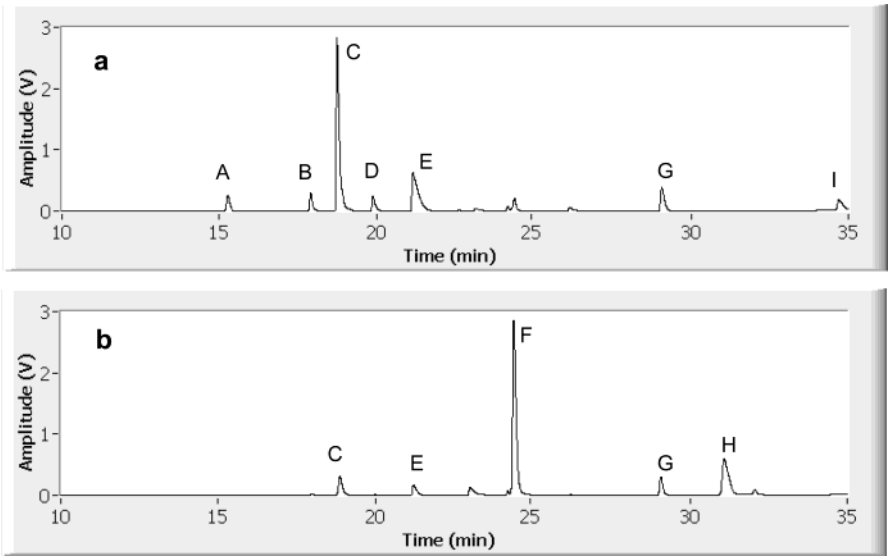

Figure 2. Representative GC-Py-GCC-IRMS pyrograms of (a) IAA at 780 °C and (b) 3MTP at 880 °C. Key: A = CH_4, B = C_2H_2, C = C_2H_4, D = C_2H_6, E = HCN, F = propylene, G = CH_3CN, H = isobutylene, and I = CS_2.

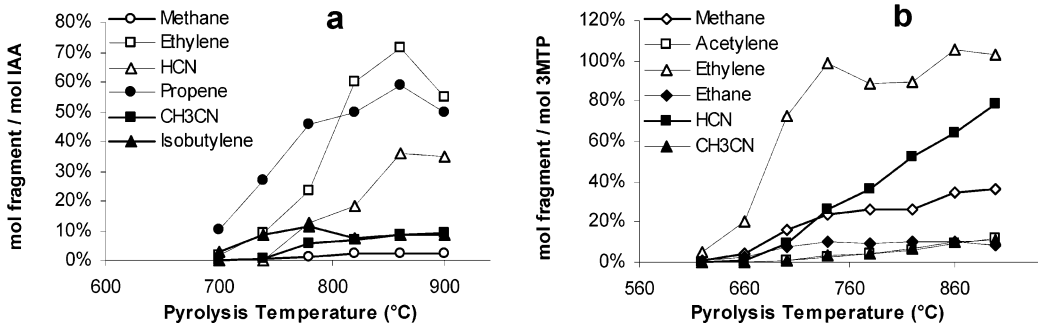

Figure 3. Pyrolysis efficiencies of (a) IAA and (b) 3MTP over a range of temperatures. The yields are expressed as the molar ratio of fragment produced divided by parent compound injected on column. Yields may be greater than 100% for fragments that can be produced from multiple locations in the parent.

weighted sum of the isotope ratios from each carbon position:

$$^{13}R_{obs} = \sum_i {}^{13}R_i[X_i] \quad (8)$$

where $^{13}R_{obs}$ is the observed isotope ratio of the fragment, $^{13}R_i$ is the isotope ratio of the ith carbon position in the parent molecule, and $[X_i]$ is the molar fraction that the ith position contributes to the fragment. If a fragment is generated completely from the ith carbon, then $[X_i] = 1.00$; if $[X_i] = 0.00$, then the ith carbon makes no contribution to the fragment.

We can separate out the contribution of the labeled carbon from the rest of the summation:

$$^{13}R_{obs} = {}^{13}R_{lab}[X_{lab}] + \sum_{i,i\neq lab} {}^{13}R_i[X_i] \quad (9)$$

A plot of $^{13}R_{obs}$ versus $^{13}R_{lab}$ should yield a straight line with slope $[X_{lab}]$, the mole fraction contribution of the labeled carbon. Plots of this nature were generated for the major pyrolysis fragments of each amino acid analogue over a range of temperatures. A representative plot for these labeling experiments is shown for the pyrolysis of 3MTP at 700 °C in Figure 4. The slope of the best-fit line for a given fragment is equal to the percent

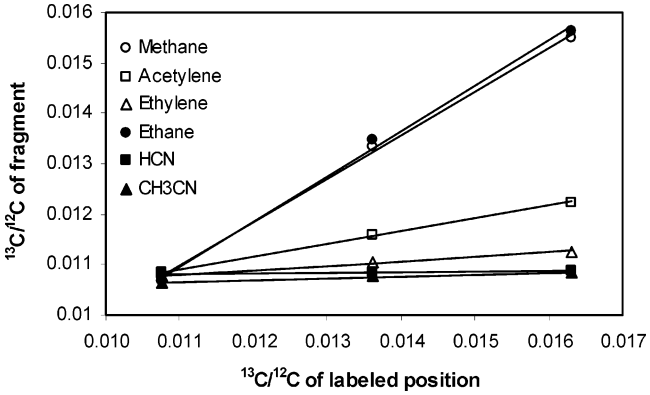

Figure 4. Representative plot of measured ^{13}R of pyrolysis fragments vs ^{13}R(C-methyl) of three standards of 3MTP enriched at different levels at the methyl position (0.0108, 0.0137, 0.0164) and pyrolyzed at 700 °C. Best-fit equations: methane (○) $y = 0.92x + 0.0008$; acetylene (□) $y = 0.17x + 0.009$; ethylene (△) $y = 0.09x + 0.01$; ethane (●) $y = 0.93x + 0.0006$; HCN (■) $y = 0.02x + 0.0107$; CH_3CN (▲) $y = 0.04x + 0.0102$; The slope of the best-fit line is equal to the mole fraction that the C(methyl) site contributes to the observed fragment; e.g., 92% of the carbon in CH_4 derives from the C(methyl).

contribution of the labeled site to the fragment. For example, 92% of the CH_4 is derived from the C(methyl) site. The percent contributions of labeled sites to pyrolysis fragments of IAA and

Table 2[a]

		temperature (°C)							
	fragment	620	660	700	740	780	820	860	900
3MTP	CH_4	99	97	92	86	80	76	71	68
	C_2H_2			17	25	31	34	35	34
	C_2H_4	4	6	9	9	12	13	14	15
	C_2H_6	99	96	93	89	87	85	85	84
	HCN		2	2	1	1	1	1	1
	CH_3CN		3	4	4	4	4	4	4
IAA	C_2H_4			25	24	22	17	16	17
	HCN					99	94	95	95
	n-C_3H_6			0	0	0	0	0	0
	i-C_4H_8			0	0	0	0	0	0
	CH_3CN				49	50	48	48	48

[a] All values are percentages. Top shows contribution of C1 position to IAA pyrolysis fragments as a function of temperature. Bottom shows contribution of C(methyl) of 3MTP to each fragment as a function of pyrolysis temperature.

3MTP are reported in Table 2. For IAA presented in Table 2, HCN originates with 99% fidelity from the C1 site at 780 °C, while propylene and isobutylene are uncontaminated with C1 carbon at all temperatures. CH_3CN is ∼50% C1 at all temperatures, as expected if there were no contamination from other sites. All three of these fragments should therefore have isotope ratios representative of their respective positions in the original molecule once properly calibrated. Similarly, Table 2 shows that CH_4, HCN, and CH_3CN will provide representative fragments for C1 analysis in 3MTP.

The major fragments appear to result from cleavage of the weakest bonds in both analogues, in accordance with Rice theory. C_2H_4 is the dominant fragment at high temperatures. In our previous PSIA studies of alcohols and *n*-alkanes, we observed both C_2H_4 and C_2H_2 as common "end-point" fragments. The same phenomenon is seen in the thermolytic cracking of aliphatic hydrocarbons. The labeling data above show that the contribution of the C(methyl) site of 3MTP and of the C1 site in IAA to the C_2H_4 and C_2H_2 fragments varies with temperature. Therefore, these fragments probably do not represent the isotopic nature of any specific location in 3MTP and thus are not useful for PSIA.

There is a modest yield of CH_4 and C_2H_6 in the pyrolysis of 3MTP but negligible amounts of these fragments in the pyrolysis of IAA. Table 2 shows that C(methyl) contributes >95% to CH_4 and C_2H_6 at low temperatures (660 °C and below). The C−S bonds of 3MTP are highly labile; the bond dissociation energy of the CH_3−S bond in methionine is estimated to be 71 kcal/mol, ∼10 kcal/mol less than the aliphatic CH_3−C bond of IAA.[25] CH_4 is therefore formed by simple homolytic cleavage of the CH_3−S bond, and C_2H_6 is a result of the recombination of methyl free radicals. As the temperature increases, the contribution of C(methyl) decreases, indicating increased contamination of the CH_4 and C_2H_6 peaks by secondary fragmentation. We chose a pyrolysis temperature of 680 °C for these two fragments as a compromise between signal size and structural fidelity.

Gas-phase pyrolysis of aliphatic primary amines is known to produce short-chain nitriles,[26] and a significant yield of HCN is observed from both analogues at temperatures above 780 °C. Labeling experiments confirm that the HCN fragment is primarily generated from the C1 carbon by simple cleavage of the CH_2−CH_2NH_2 bond. There is a negligible contribution of the labeled C(methyl) site of 3MTP, as expected. Labeling experiments on IAA show 94−98% contribution of the C1 carbon to the HCN fragment over a temperature range of 780−900 °C.

Both analogues produce a modest yield of CH_3CN at temperatures above 780 °C. This fragment is primarily formed by cleavage between the C2 and C3 carbons. The C1 position of IAA contributes ∼50% to the CH_3CN fragment at 780 °C, which is expected if the fragment was formed solely by single bond cleavage. However, in the pyrolysis of 3MTP, the C(methyl) site shows a steady 4% contribution to the CH_3CN fragment over a wide range of temperatures. The mechanism for this is likely a recombination between $CH_3^{\bullet}$ and $^{\bullet}CH_2NH_2$ free radicals.

In IAA, the formation of the HCN and CH_3CN fragments results in the generation of corresponding isobutylene (C_4H_8) and propylene (C_3H_6) fragments in very good yield (20 and 60%, respectively, at 860 °C). The C1 carbon did not contribute to either fragment over a wide range of temperatures, so both fragments are likely generated by simple homolytic cleavage.

Pyrograms of 3MTP do not show evidence of $CH_3SC_2H_5$ or CH_3SCH_3, the corresponding fragments of HCN and CH_3CN. If aliphatic S-containing radicals are formed, further cleavage is probably favored over recombination with hydrogen or other free radicals due to the fragile nature of the C−S bonds. Sulfur is detected in the pyrograms in the form of CS_2 and H_2S. The origin of the carbon in the CS_2 fragment is unclear, and therefore, the fragment is not useful for PSIA studies.

In summary, each analogue produced four pyrolysis fragments of acceptable yield and fidelity to be useful for PSIA. For 3MTP, these fragments are CH_4 and C_2H_6 at 680 °C, which derive from the C(methyl) group; HCN at 780−900 °C, which derives from the C1 position; CH_3CN at 780−900 °C, which derives 50% from C1, 46% from C2 position, and 4% from C(methyl). These fragments enable the calculation of $\Delta\delta^{13}C$ at every position in 3MTP via the following equations:

$$\Delta\delta^{13}C(C1) = \Delta\delta^{13}C(HCN) \quad (10a)$$

$$\Delta\delta^{13}C(C2) = (\Delta\delta^{13}C(HCN) - 0.04\Delta\delta^{13}C(C1) - 0.5\Delta\delta^{13}C(C_1 - \text{methyl}))/0.46 \quad (10b)$$

$$\Delta\delta^{13}C(C3) = \Delta\delta^{13}C(\text{Total}) - (\Delta\delta^{13}C(C1) + \Delta\delta^{13}C(C2) + \Delta\delta^{13}C(C_1 - \text{methyl}))/4 \quad (10c)$$

$$\Delta\delta^{13}C(C_1 - \text{methyl}) = \Delta\delta^{13}C(C_2H_6) \quad (10d)$$

For IAA, useful fragments are HCN above 780 °C, which derives from the C1 position; CH_3CN, which derives from the C1and C2 position; propylene, which derives from the propyl group; and isobutylene, which derives from the C2 position and the propyl group. These fragments enable the calculation of $\Delta\delta^{13}C$ for the C1 and C2 positions and the propyl moiety of IAA by the

(25) McMillen, D. F.; Golden, D. M. *Annu. Rev. Phys. Chem.* **1982**, *33*, 493−532.

(26) Lovas, F. J.; Clark, F. O.; Tiemann, E. *J. Chem. Phys.* **1975**, *62*, 1925−1931.

Table 3. Absolute ($\delta^{13}C_{Pdb}$) and Relative ($\Delta\delta^{13}C_N$) Isotope Ratios of 3MTP Pyrolysis Fragments (T = 880°C)

		fragment				
source		CH_4	C_2H_6	HCN	CH_3CN	CSIA[a]
E	$\delta^{13}C_{pdb}$	−49.18 ± 0.58	−53.43 ± 0.06	−29.16 ± 0.39	−24.76 ± 0.22	−24.07± 0.17
	$\Delta\delta^{13}C_H$	2.04 ± 0.70	2.75 ± 0.31	13.22 ± 0.42	25.03 ± 0.27	13.96 ± 0.33
F	$\delta^{13}C_{pdb}$	−46.20 ± 0.53	−50.82 ± 0.43	−26.08 ± 0.14	−19.19 ± 0.16	−20.43 ± 0.12
	$\Delta\delta^{13}C_H$	5.02 ± 0.65	5.36 ± 0.53	16.30 ± 0.22	30.60 ± 0.22	17.59 ± 0.31
G	$\delta^{13}C_{pdb}$	−46.42 ± 0.46	−51.33 ± 0.31	−26.14 ± 0.11	−19.85 ± 0.06	−20.71 ± 0.12
	$\Delta\delta^{13}C_H$	4.79 ± 0.60	4.86 ± 0.46	16.24 ± 0.20	29.94 ± 0.17	17.32 ± 0.31
H	$\delta^{13}C_{pdb}$	−51.21 ± 0.38	−56.18 ± 0.31	−42.37 ± 0.16	−49.79 ± 0.16	−38.03 ± 0.28
	$\Delta\delta^{13}C_H$	0	0	0	0	0

[a] CSIA refers to $\delta^{13}C$ and $\Delta\delta^{13}C_H$ of the total compound.

Table 4. Absolute ($\delta^{13}C_{pdb}$) and Relative ($\Delta\delta^{13}C_N$) Isotope Ratios of IAA Pyrolysis Fragments (T = 780 °C)

		fragment				
source		n-C_3H_6	i-C_4H_8	HCN	CH_3CN	CSIA[a]
L	$\delta^{13}C_{pdb}$	−29.59 ± 0.06	−27.98 ± 0.31	−29.24 ± 0.40	−19.43 ± 0.17	−25.49 ± 0.19
	$\Delta\delta^{13}C_N$	−8.28 ± 0.09	−5.68 ± 0.20	−9.69 ± 0.69	−0.55 ± 0.17	−5.66 ± 0.27
M	$\delta^{13}C_{pdb}$	−20.64 ± 0.19	−22.11 ± 0.10	−36.62 ± 0.21	−27.94 ± 0.44	−29.39 ± 0.19
	$\Delta\delta^{13}C_N$	0.67 ± 0.19	0.20 ± 0.27	−17.06 ± 0.61	−9.06 ± 0.44	−3.90 ± 0.27
N	$\delta^{13}C_{pdb}$	−21.31 ± 0.07	−22.31 ± 0.25	−19.55 ± 0.57	−18.88 ± 0.44	−31.14 ± 0.20
	$\Delta\delta^{13}C_N$	0	0	0	0	0

[a] CSIA refers to $\delta^{13}C$ and $\Delta\delta^{13}C_N$ of the total compound.

following equations:

$$\Delta\delta^{13}C(C1) = \Delta\delta^{13}C(HCN) \quad (11a)$$

$$\Delta\delta^{13}C(C2) = 2(\Delta\delta^{13}C(CH_3CN) - 0.5\Delta\delta^{13}C(C1)) \quad (11b)$$

$$\Delta\delta^{13}C(propyl) = \Delta\delta^{13}C(propene) \quad (11c)$$

Comparison of Fragment $\Delta\delta^{13}C$ from Multiple Sources. $\delta^{13}C_{pdb}$ values calibrated against CO_2 gas for the CH_4 and C_2H_6 fragments, generated at 680 °C, and the HCN and CH_3CN fragments, generated at 880 °C, are reported for the four sources of 3MTP in Table 3. $\delta^{13}C_{pdb}$ values of the C_3H_6, C_4H_8, HCN, and CH_3CN fragments, all generated at 780 °C, are reported for the three sources of IAA in Table 4. The $\delta^{13}C_{pdb}$ of the total carbon in each source, as measured by GCC−IRMS, is also reported. As was discussed earlier, the $\delta^{13}C$ values of the observed fragments calibrated against CO_2 gas may not be equal to the isotope ratios of the corresponding position(s) on the original source due to pyrolysis-induced fractionation. Thus, $\Delta\delta^{13}C$ are also calculated from $\delta^{13}C_{pdb}$ to emphasize relative isotope ratios.

The average precision for fragments from both 3MTP and IAA was SD($\delta^{13}C$) < 0.3‰. Even allowing for a sizable fractionation factor of 5−10‰, the CH_4 fragment, and hence the terminal C(methyl) carbon, is clearly depleted in all 3MTP sources ($\delta^{13}C_{pdb}$ = −45 to −51‰). In sources derived from methionine (E, F, G), C(methyl) is markedly depleted with respect to the total carbon of the source ($\delta^{13}C_{pdb} \sim -20$‰). If our commercial source of methionine is from a biological source, this may reflect fractionation of the terminal methyl as a result of methionine's role in the one-carbon pool. The disparity between the C(methyl) carbon and the other fragments is much smaller in source H. This may indicate that the commercial 3MTP is not derived from a biological source, but instead synthesized by a nonnatural method. Unfortunately, manufacturers generally consider information about sources proprietary, and they were not able to discuss with us the origin of their sources in detail.

We calculated $\Delta\delta^{13}C$ values as described in eq 7. Source N (IAA) and source H (for 3MTP) were arbitrarily chosen as standards. $\Delta\delta^{13}C_H$ (Table 3) and $\Delta\delta^{13}C_N$ (Table 4) of the pyrolysis fragments are reported. By definition, $\Delta\delta^{13}C_H$ of H and $\Delta\delta^{13}C_N$ of N equals zero for any fragment. The average precision for the $\Delta\delta^{13}C$ measurements was SD($\Delta\delta^{13}C$) < 0.5‰ for both IAA and 3MTP. This is slightly worse than the precision for the $\delta^{13}C$ values, due to propagation of errors.

The utility of the $\Delta\delta^{13}C$ notation over $\delta^{13}C$ is evident when we study the invariance of $\Delta\delta^{13}C$ to changes in pyrolysis temperature. We determined $\delta^{13}C_{pdb}$ and $\Delta\delta^{13}C_H$ for the HCN and CH_3CN fragments of all 3MTP sources at 800, 840, and 880 °C, and $\delta^{13}C_{pdb}$ and $\Delta\delta^{13}C_N$ for the HCN, CH_3CN, and C_3H_6 fragments for all IAA sources at 780, 800, 820, and 840 °C. Plots of the dependency of $\Delta\delta^{13}C$ and $\delta^{13}C$ with respect to temperature are shown in Figure 5 for two of the fragments, HCN and propylene from the IAA parent. In all cases, $\Delta\delta^{13}C$ is less dependent on temperature than $\delta^{13}C$. The average range of $\Delta\delta^{13}C$ for a fragment over the measured temperature range was only 0.5‰. Eleven of the 12 fragments did not show a significant variation (p < 0.05) in $\Delta\delta^{13}C$ values over the observed temperature ranges. In contrast, the average range of $\delta^{13}C_{pdb}$ was 1.6‰, and only one fragment *did not* show a significant variation (p < 0.05) in $\delta^{13}C_{pdb}$ as temperature was varied.

Isotope ratios of complementary fragments of IAA further indicate that $\Delta\delta^{13}C$ is well suited for reporting intramolecular isotope values. Complementary fragments, introduced in a PSIA studies of hydrocarbons,[7] are defined as two fragments that contain all the carbon positions in the parent molecule. Two pairs

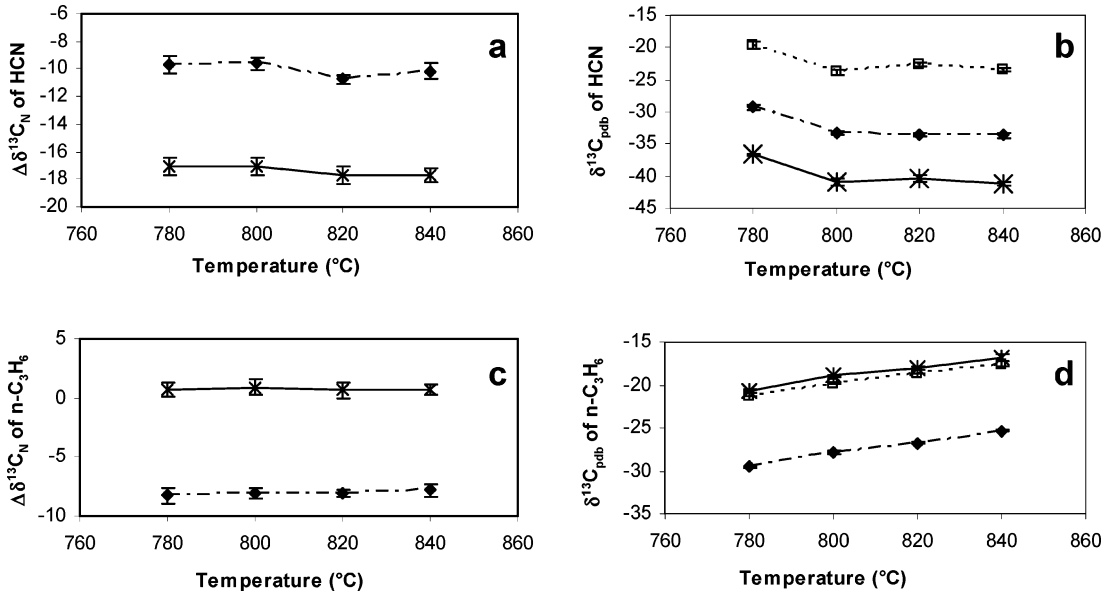

Figure 5. Dependence of (b) δ^{13}C and (a) $\Delta\delta^{13}$C of HCN, and (d) δ^{13}C and (c) $\Delta\delta^{13}$C of propylene fragments, from IAA on pyrolysis temperature. Relative isotope ratios ($\Delta\delta^{13}C_N$) are much more invariant to changing pyrolysis temperature than absolute isotope ratios (δ^{13}C). Key to sources: L (◆); M (×); N (□).

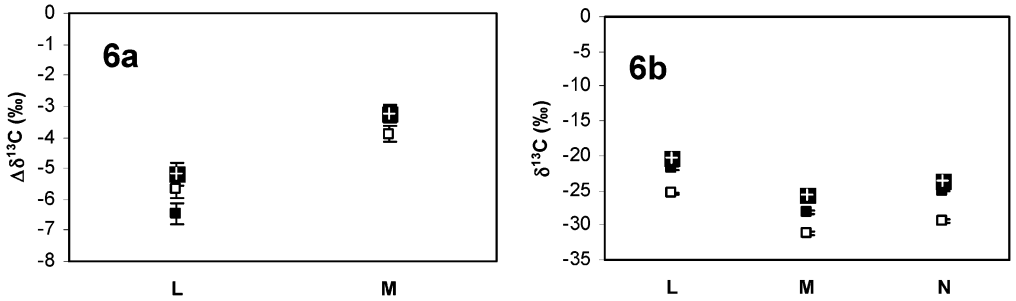

Figure 6. (a) $\Delta\delta^{13}C_N$ and (b) δ^{13}C values of total carbon of IAA reconstructed from complementary fragments, compared to total carbon as measured by GCC−IRMS. Error bars for δ^{13}C values are mostly within the data points. Key: closed square, HCN + isobutylene; open square, CH_3CN + propylene; crossed square, total measured by CSIA.

of complementary fragments exist for IAA: (CH_3CN, C_3H_6) and (HCN, C_4H_8). If the complementary fragments are formed without competing pathways, then the weighted averages of the $\Delta\delta^{13}C_N$ values should add to make the $\Delta\delta^{13}C_N$ values of the total compound by the following equation:

$$\Delta\delta^{13}C_N(\text{Total}) = F_A\Delta\delta^{13}C_N(A) + F_B\Delta\delta^{13}C_N(B); \quad F_A + F_B = 1 \quad (12)$$

where F_x is the mole fraction contribution of complementary fragment X. If the complementary fragments are formed without fractionation, then the weighted averages of the $\delta^{13}C_{pdb}$ values should be additive:

$$\Delta\delta^{13}C\ (\text{Total}) = F_A\delta^{13}C\ (A) + F_B\Delta\delta^{13}C(B); \quad F_A + F_B = 1 \quad (13)$$

Figure 6a shows $\Delta\delta^{13}$C of the total carbon in IAA as measured by CSIA and reconstructed from complementary fragments generated at 780 °C. There is excellent agreement between the reconstructed and CSIA measurements; the reconstructed $\Delta\delta^{13}$C is within 0.8‰ of the CSIA value for all four pairs, and the differences were not significant ($p < 0.05$).

Figure 6b shows raw δ^{13}C of the total carbon in IAA as measured by CSIA and as reconstructed from complementary fragments generated at 780 °C. In contrast to the $\Delta\delta^{13}$C results, the reconstructed δ^{13}C values were enriched by 3−5‰ with respect to the CSIA value and were significant ($p < 0.05$) for all complementary fragments. Changing the pyrolysis temperature did not improve this agreement.

The labeled 3MTP studies indicate that CH_4 and C_2H_6 derive their carbon primarily from the C(methyl) group. Therefore, we expect that $\Delta\delta^{13}C_H(CH_4)$ and $\Delta\delta^{13}C_H(C_2H_6)$ should be the same for any one sample. At a pyrolysis temperature of 680 °C, the difference between $\Delta\delta^{13}C_H(CH_4)$ and $\Delta\delta^{13}C_H(C_2H_6)$ ranges from 0.71‰ for E to 0.07‰ for G (Table 4), and the differences are not significant. Because CH_4 and C_2H_6 derive from the same carbon site, the difference between their isotope ratios is invariant at constant pyrolysis conditions, although their absolute isotope ratios ((δ^{13}C) differ by 4−5‰. We conclude that $\Delta\delta^{13}$C are robust representations of relative carbon isotope ratios.

We used $\Delta\delta^{13}C_H$ values of fragments from and mass balance to calculate the $\Delta\delta^{13}C_H$ values of individual carbon sites, presented

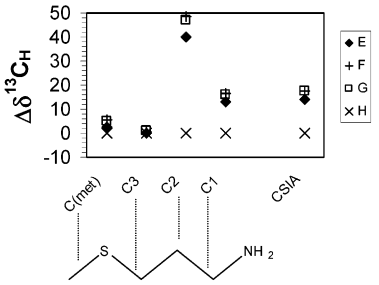

Figure 7. $\Delta\delta^{13}C_H$ for all four carbon positions of 3MTP at $T = 880$ °C. $\Delta\delta^{13}C_H = \delta^{13}C(\text{Sample}) - \delta^{13}C(\text{Source H})$ for a given fragment. By definition, $\Delta\delta^{13}C_H = 0$ for all fragments and positions from source H.

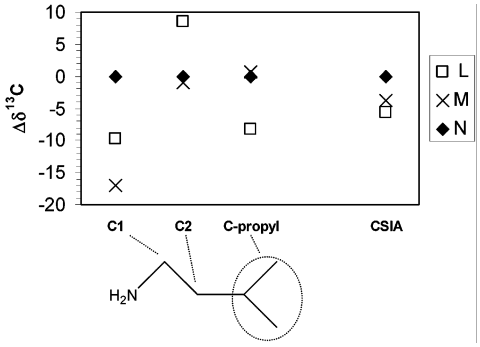

Figure 8. $\Delta\delta^{13}C_N$ for C1, C2, and propyl moiety of IAA at $T = 780$ °C. $\Delta\delta^{13}C_N = \delta^{13}C(\text{Sample}) - \delta^{13}C(\text{Source N})$ for each a given fragment. By definition, $\Delta\delta^{13}C_N = 0$ for all fragments and positions from source N.

in Figure 7. The variation at each position is greater than is normally seen in, for instance, C3/C4 photosynthetic fractionation. Most striking, the C2 position is enriched by +48.33‰ in source F compared to H. In fact, all three of the 3MTP sources derived from methionine were enriched by at least 39‰ at the C2 position. This difference is even more remarkable considering that no other position shows a difference of >20‰ compared to source H. In fact, $\Delta\delta^{13}C_H$(C3) is not significantly different from 0‰ for any of the three sources. The enhanced utility of PSIA over CSIA is very evident in these data. Using CSIA, we could determine only that the three sources of 3MTP derived from methionine (E, F, G) were enriched by 14−18‰ with respect to H. With PSIA, we see that this enrichment is concentrated primarily in the C2 position (39−48‰), with minor enrichment in the C1 position (13−16‰) and C(methyl) position (3−5‰). The similarity of $\Delta\delta^{13}C_H$ values for F and G at each position suggests that the methionine purchased from Avocado and Acros Organics was drawn from the same source.

Analogously, we used $\Delta\delta^{13}C_N$ of the fragments to calculate the $\Delta\delta^{13}C_N$ values of individual carbon sites in IAA (Figure 8). Unfortunately, because the CH_4 fragment was not formed in significant yield, we could not distinguish the isotope ratio of the two CH_3 groups from the C3 position; instead, we report $\Delta\delta^{13}C_N$-(propyl), the intramolecular isotope ratio of the propyl fragment. The variation is not as dramatic as between the sources of 3MTP. M is depleted by ∼−3.6‰ compared to N in CSIA. However, PSIA shows that M is *enriched at C(propyl)* by 0.7‰, and is *depleted at C1* by −17.1‰, compared to the N standard. A similar trend is seen with source L, where $\Delta\delta^{13}C_N$(C1) = −9.7‰ and $\Delta\delta^{13}C_N$(C2) = 8.6‰. Without knowing the origins of each source, other than the name of the manufacturer, it is difficult to draw conclusions on why these differences exist. However, the three sources of IAA are clearly distinguishable.

Experimental and Theoretical Limits of Sample Size. The typical lower limit of analyte require to yield precision of SD(δ^{13}C) < 0.3‰ is ∼10 ng of C on-column in continuous-flow IRMS using the conventional summation algorithm for data reduction. Using curve fitting to improve data reduction, we routinely achieve precision of SD($\delta^{13}C_{pdb}$) < 0.5‰ for 500 pmol of C on column. Pyrolysis efficiency in GC-Py-GCC-IRMS is much less than 100% for some fragments, so the fragment formed in the poorest yield limits the minimum sample size. For 3MTP, the limiting fragment is C_2H_6, which is formed with a pyrolysis efficiency of ∼5% at 680 °C. A yield of 500 pmol of CH_4 requires 10 nmol, or 1 μg, of 3MTP on column. In our own experimental work, we operated within a factor of 2 of this limit. The limiting fragment in the pyrolysis of IAA is CH_3CN, which is formed with a yield of ∼6%. Since every mole of CH_3CN produces 2 mol of C, we should need only 250 pmol of CH_3CN postpyrolysis; this requires 4.2 nmol, or 0.4 ng, of IAA.

CONCLUSIONS

We have demonstrated that on-line pyrolysis of two amino acid analogues, 3MTP and IAA, generates characteristic fragments with reproducible $^{13}C/^{12}C$ isotope ratios (SD($\delta^{13}C_{pdb}$) < 0.3‰). Relative isotope ratios, $\Delta\delta^{13}C$, were calculated either directly or by mass balance for all four carbon positions of 3MTP and for two of the carbon positions and the propyl group of IAA. Our PSIA studies highlight the intramolecular variability of isotope ratios and also indicate that a great deal of information is lost in compound-specific analyses. For example, two unique sources of 3-methylpropylamine differed by 17.3‰ by CSIA, but our PSIA work on the same two sources shows a difference of 48.3‰ at C2 and 1‰ at C3. The system is well suited to study small, biologically relevant, kinetic isotope effects at specific sites of small molecules that would otherwise be obscured by CSIA studies. These techniques may be useful for correlating subtle changes in intramolecular isotope ratios to physiological events or stresses.

Our data provide strong evidence that $\Delta\delta^{13}C$ is conserved throughout pyrolysis, as expected on theoretical grounds. In our work, $\Delta\delta^{13}C$ values of fragments are invariant for a given set of pyrolysis conditions. The $\Delta\delta^{13}C$ values measured by CSIA were identical to those reconstructed from the $\Delta\delta^{13}C$ values of complementary fragments, and different fragments formed from the same site within a parent compound have identical $\Delta\delta^{13}C$ values.

Sample size in our work is limited primarily by fragment pyrolysis efficiencies as low as 5% and therefore requires 1−2 orders of magnitude more sample than CSIA on the same compound. In future refinements, pyrolysis efficiency might be raised while still minimizing the degree of secondary fragmentation. This could be accomplished by altering the residence time of the analyte within the heated pyrolysis zone or by turning to new methods of fragmentation such as laser-induced pyrolysis.

ACKNOWLEDGMENT

This work was funded by NIH Grant GM49209.

Received for review May 8, 2003. Accepted July 21, 2003.

AC0344889